General

All chemicals, unless otherwise stated, were purchase from Sigma Aldrich and were used as received. All instruments were calibrated and maintained in accordance with previously reported routine quality-control procedures (*1*). Radioactivity measurements were made using a CRC-15R dose calibrator (Capintec). For accurate quantification of radioactivity, experimental samples were counted for 1 min on a calibrated Cobra 5003 γ-counter (Packard Instruments) using a dynamic energy window of 650–1,000 keV for ^{89}Zr (909-keV emission). ^{89}Zr-radiolabeling reactions were monitored using silica-gel impregnated glass-fiber instant thin-layer chromatography (iTLC-SG) paper (Varian Inc.) and analyzed on a Cyclone Plus phosphor imager (Perkin Elmer). Diethylene triamine pentaacetic acid in water (DTPA, 50 mM, pH 7) was used as a mobile-phase solvent. Additionally, the chemical and radiochemical purity of crude and purified radiolabeled antibodies was assessed by HPLC using an ENrich size exclusion column (Bio-Rad) with PBS/DTPA (1 mM; pH 7.4) as a mobile-phase solvent at a flow rate of 1.25 mL/min.

Radioactivity

To measure the specific activity of ^{89}Zr-oxalate, ^{89}Zr-oxalate stock solution (120 μL; ∼150–200 MBq) was added to 1.2 mL of 0.25 M HEPES and the pH was adjusted to 7–8 using 1.0 M NaOH. Then, 100-μL samples derived from a 1:3 serial dilution of desferrioxamine B in 18.0 MΩ water (ranging from 10 μg/mL to 1.5 ng/mL [15.2 nmol–2.3 pmol]) were added to 1.0-mL Eppendorf tubes before adding a standard amount of ^{89}Zr-oxalate in HEPES buffer (100 μL; ∼10 MBq). Water blank reactions were used as controls. Reactions were incubated at room temperature (RT) for more than 1 h, after which time the reactions were quenched for 15 min at RT by the addition of DTPA (50 μL; 50 mM; pH 7.4). Then, 1-μL aliquots were removed from each vial, spotted on iTLC-SG glass strips, and developed using a DTPA (50 mM; pH 7.4) mobile phase. Activity at the solvent front (R_f = 1.0; corresponding to ^{89}Zr-DTPA) and baseline (R_f = 0.0; corresponding to ^{89}Zr-DFO) was measured on a Cyclone Plus phosphor imager (Perkin Elmer). For accurate quantification of radioactivity, iTLC plates were cut in half (at R_f = 0.5) and the two sections were counted using a calibrated and normalized γ-counter.

Cell Lines

The human anaplastic large cell lymphoma (ALCL) cell line Karpas 299 was obtained from Sigma-Aldrich. Karpas 299 cells were grown in RPMI-1640 medium, supplemented with 10% fetal calf serum (FCS; Life Technologies GmbH), and 100 units/mL of both penicillin and streptomycin. A-431 cells were grown in Dulbecco modified Eagle medium (DMEM), containing 10% fetal bovine serum, and 100 units/mL of both penicillin and streptomycin. Cell lines were maintained in a 5% CO_2(g) atmosphere at 37°C.

Xenograft Models

All animal experiments were conducted according to the regulations of the University Medical Center of Freiburg, Germany. Female BALB/c nude mice (18–20 g, 6–8 wk old) were obtained from Janvier SAS. Mice were provided with food and water ad libitum. Karpas 299 tumors were induced on the shoulder by subcutaneous (s.c.) injection of 20.0–25.0 million cells in a 100-μL cell suspension of a 1:1 v/v mixture of medium with reconstituted basement membrane (GFR BD Matrigel; Corning BV). Similarly, A-431 tumors were induced on the shoulder by s.c. injection of 5.0 million cells. Palpable Karpas 299 tumors developed after 14–21 d. A-431 tumors grew more rapidly with more uniform size distribution and were suitable for use for in vivo studies after 10–14 d. The tumor volume (V/mm^3) was estimated by external vernier caliper measurements of the longest axis, a/mm, and the axis perpendicular to the longest axis, b/mm. The tumor volume was calculated in accordance with the equation $V = ab^2/2$.

Biodistribution Studies

Biodistribution studies were conducted to evaluate the uptake of ^{89}Zr-DFO-AC-10 in mice bearing s.c. Karpas 299 or A-431 tumors. Mice were randomized before the study and were warmed gently with a heat lamp 5 min before receiving ^{89}Zr-DFO-AC-10 (0.55–0.74 MBq, 8 μg of mAb in 100 μL of 0.9% sterile saline for injection) via intravenous (i.v.) tail-vein injection (t = 0 h). Animals (n = 3–4, per group) were euthanized by asphyxiation with excess isoflurane at 24, 72, and 144 h after injection, and 12 tissues (including the tumor) were removed, rinsed in water, dried in air for 5 min, weighed, and counted on a γ-counter for accumulation of ^{89}Zr radioactivity. Count data were background- and decay-corrected, and the percentage injected activity per gram (%IA/g) for each tissue sample was calculated by normalization to the total

amount of activity injected. The total counts injected per mouse were determined by application of a measured calibration factor using known standards.

Blocking studies were also performed in vivo to investigate the specificity of ^{89}Zr-DFO-AC-10 for CD-30. Nonradiolabeled AC-10 (~25 mg/kg solution with sterile saline; 0.5 mg/mouse; ~64-fold excess) was injected 5–10 min before the ^{89}Zr-DFO-AC10 (8 μg/mAb per mouse), and biodistribution studies were performed at 72 h after i.v. administration (n = 3).

Small-Animal PET/CT Imaging

PET imaging experiments were conducted on a microPET Focus 120 scanner (Concorde Microsystems) (*2*). Mice were administered ^{89}Zr-DFO-AC-10 formulations (6.9–7.5 MBq, 80–82 μg of mAb in 100 μL of 0.9% sterile saline for injection) via tail-vein injection. Approximately 5 min before recording of the PET images, the mice were anesthetized by inhalation of 2%–3% isoflurane/oxygen gas mixture and placed on the scanner bed in the prone position. Anesthesia was maintained using 1%–2% isoflurane. PET images were recorded at various time points between 24 and 144 h after injection. List-mode data were acquired for between 10 and 30 min using a γ-ray energy window of 350–650 keV and a coincidence timing window of 6 ns. For all static images, scan time was adjusted to ensure that a minimum of 15 million coincident events were recorded. PET sinograms were reconstructed after Fourier rebinning using a 2-dimensional ordered-subset expectation maximization (2D-OSEM) algorithm. Image counts per pixel per second were calibrated to activity concentrations (Bq/mL) by measuring a 3.5-cm cylinder phantom filled with a known concentration of radioactivity. The PET and CT images of the animal studies were coregistered using the Rover software (ABX). For quantification of tumor radioactivity uptake in the static PET scans, small 3-dimensional volumes of interest (VOIs) were drawn using AMIDE Medical Image Data Examiner software (*3*), and the mean %IA/g (decay-corrected to the time of injection) in various tissues was determined.

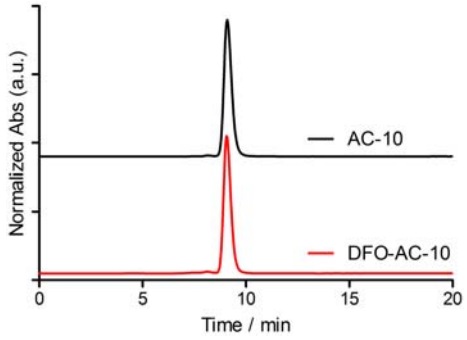

Supplemental Figure 1. HPLC chromatograms of AC-10 and DFO-AC-10. Electronic absorption (λ = 280 nm) showing the chemical purity of AC-10 and conjugated DFO-AC-10 antibody.

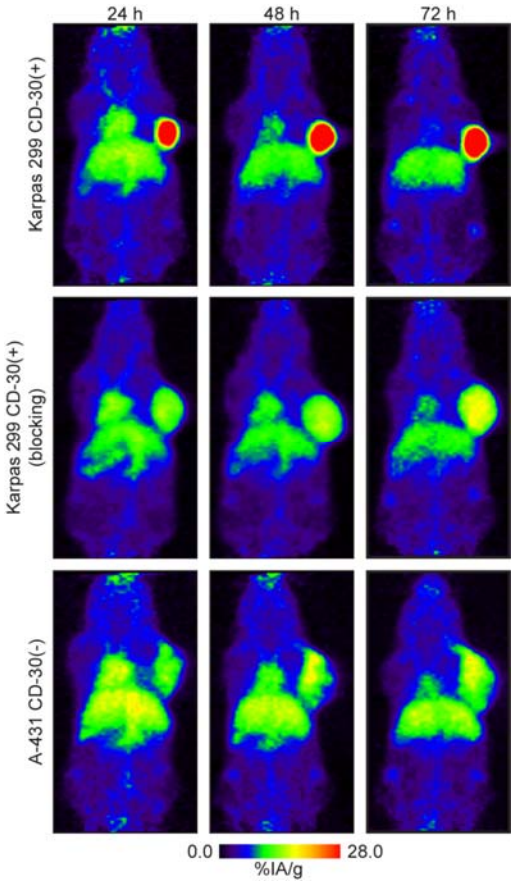

Supplemental Figure 2. MIP PET images recorded in tumor-bearing mice at 24–72 h after administration of ^{89}Zr-DFO-AC-10 (20 μg mAb; 2.3 MBq; 100 μL) in (top) a CD30(+) Karpas 299 model, (middle) a CD30(+) Karpas 299 model blocked with excess AC-10 (65-fold excess), and (bottom) a CD30(–) A-431 model.

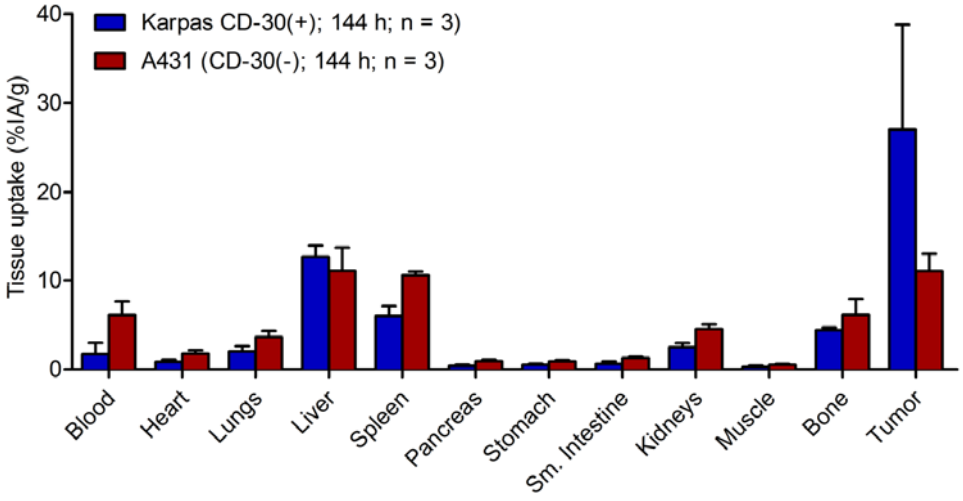

Supplemental Figure 3. Biodistribution data 144 h after final PET/CT imaging time point.

Supplemental Table 1. Biodistribution data 144 h after administration of ^{89}Zr-DFO-AC-10 (~80 μg mAb) by tail-vein injection to female BALB/c nude mice bearing s.c. CD30(+) Karpas 299 or CD30(–) A-431 tumors

	A-431 CD30(–)	**Karpas 299 CD30(+)**
Tissue	144 h (*n* = 3)	144 h (*n* = 3)
Blood	6.08 ± 1.55	1.70 ± 1.29
Heart	1.75 ± 0.39	0.83 ± 0.26
Lung	3.62 ± 0.72	2.00 ± 0.60
Liver	11.06 ± 2.72	12.65 ± 1.38
Spleen	10.57 ± 0.41	6.00 ± 1.11
Pancreas	0.92 ± 0.19	0.41 ± 0.12
Stomach	0.90 ± 0.14	0.51 ± 0.12
Small intestine	1.28 ± 0.15	0.60 ± 0.28
Kidney	4.55 ± 0.51	2.48 ± 0.47
Muscle	0.52 ± 0.09	0.28 ± 0.14
Bone	6.12 ± 1.78	4.40 ± 0.32
Tumor	11.02 ± 1.96	27.02 ± 11.73
Tumor/blood	1.81 ± 0.56	15.93 ± 13.94
Tumor/liver	1.00 ± 0.30	2.14 ± 0.96
Tumor/spleen	1.04 ± 0.19	4.51 ± 2.13
Tumor/kidney	2.43 ± 0.51	10.90 ± 5.17
Tumor/muscle	21.24 ± 5.32	95.68 ± 62.47
Tumor/bone	1.80 ± 0.62	6.15 ± 2.71

Data are mean %IA/g ± SD. Errors for tumor-to-tissue ratios are geometric mean of SDs. Data were obtained on mice used for PET/CT imaging.

References

1. Zanzonico P. Routine quality control of clinical nuclear medicine instrumentation: a brief review. *J Nucl Med.* 2009;49:1114–1131.
2. Kim JS, Lee JS, Im KC, et al. Performance measurement of the microPET Focus 120 scanner. *J Nucl Med.* 2007;48:1527–1535.
3. Loening A, Gambhir S. AMIDE: a free software tool for multimodality medical image analysis. *Mol Imaging.* 2003;2:131–137.